

MAGNETIC MOMENT MEASUREMENT OF BARYONS WITH HEAVY-FLAVORED QUARKS BY PLANAR CHANNELING THROUGH A BENT CRYSTAL

Ick Joh KIM

Physics Department, SUNYA, Albany, NY 12222, USA

Received 26 November 1982
(Revised 13 June 1983)

The precession angle of a polarization vector is calculated for a positively charged short-lived baryon channeling between single-crystal planes. When very energetic polarized baryons are produced such that the production plane of the baryon is almost parallel to the crystal plane, it is shown that the interaction of the polarization with inhomogeneous electric fields inside the crystal can be neglected from the equation of motion of the particle. In this case, the equation of motion of the polarization vector becomes the same as when the electric field is homogeneous. It is also shown that when the crystal is bent perpendicular to the planar direction, the precession angle of the polarization vector of short-lived baryons can be expressed as $\Delta\theta_R^* = \frac{1}{2}\gamma^2[(2 - g + g/\gamma^2)]v\tau/R$ under the same condition as above, where γ is the Lorentz factor, g the g factor of the magnetic moment, R the bending radius of the crystal and τ the lifetime of the particle. It is also shown that in some cases this precession should be large enough to determine the magnetic moment of short-lived particles, such as the charmed baryon Λ_c^+ .

1. Introduction

The magnetic moment of baryons, which is related to the spin vector by the formula $\mu = (gq/2mc)S$, where q is the charge, S the spin and m the mass of the particle, is one of the most important intrinsic properties of elementary particles and the possibility of measuring it has been first discussed by Goldhaber [1] and by Lee and Yang [2]. The g factor is 2 for a charged point-like Dirac particle, and $g = 0$ for a spin- $\frac{1}{2}$ neutral particle. Deviation from these values, usually called the anomalous magnetic moment, is interpreted as evidence of hadronic substructure. The simple quark model [3–7] fits reasonably well most of the existing data on the magnetic moments of baryons with $g = 2$ for quarks (table 1), which include the light quarks u, d and strange quark s . This fact has been seen as clear evidence supporting the view that quarks indeed behave as point-like Dirac particles.

Recent precise measurements of baryonic magnetic moments [8–11] have significantly improved the accuracy and triggered several new attempts at theoretical studies [12–15]. Although overall agreement between theoretical predictions and

TABLE 1
Magnetic moments of baryons (units in $\mu_N = eh/2m_p c$)

Particles	Theory [41]	Experiments	Ref.
p	2.79	2.79	
n	-1.91	-1.91	
Λ	-0.612	-0.6129 ± 0.0045	[9]
Σ^+	2.39	2.33 ± 0.13	[42]
Σ^-	-0.95	-1.40 ± 0.37	[43]
Σ^0	0.61		
Ξ^0	-1.27	-1.250 ± 0.014	[9]
Ξ^-	-0.48	-0.75 ± 0.07	[44]
$\Lambda\Sigma^0$	1.45	$1.82^{+0.25}_{-0.18}$	[45]

experimental data has improved, none of the present models fit all the available data satisfactorily. In particular for the magnetic moment of Σ^- and Ξ^- the agreement is poor. Moreover, there are many different models and unresolved ambiguities related to quark ordering.

Recently, the possible substructure of the quark is actively discussed and accurate knowledge of the magnetic moments of baryons and quarks could play a very important role in testing these ideas and could impose significant constraints on any model proposed [16, 17]. Since the discovery of the J/ψ particle, many new particles with heavy flavored quarks, namely charm and bottom quarks, have been discovered, revealing new physical phenomena. Unfortunately, however, there are no experimental data available on the magnetic moment of baryons with heavier flavored quarks. Such information obviously introduces a new dimension and should be accounted for by any comprehensive hadronic theory. This would also help to eliminate quark ordering ambiguities in the theoretical models. A reason of the non-availability of experimental information on the magnetic moments of baryons with heavy flavored quarks is because their lifetimes are too short to measure the magnetic moment by standard techniques. There is also an overall lack of understanding of the hadronic production mechanism, decay channels etc.

One of the typical methods applied to determine the baryonic magnetic moment is to measure the precession angle of the polarization vector of the particles in a known magnetic field by analysing the proton emission angular distribution in the final decaying states [9]. However, the lifetime of the baryons, which have heavier flavored quarks as their constituents, like Λ_c^+ , is too short for a conventional magnet to produce any detectable effect on the polarization vector of the particles before they decay. Typically the lifetime of Λ_c^+ is of the order of 10^{-13} sec, which results in $c\tau \sim 0.003$ cm. Therefore, it is desirable to search for an alternative to measure the magnetic moment of short-lived baryons. A potential candidate is to use a strong electric field inside a single crystal of high atomic number. This was first pointed out in 1980 by Pondrom.

In this report we study the motion of channeling particles and the equation of the polarization vector under the influence of the crystal electric field and investigate the effect of the electric field of the planes and axes of different available crystals. This study shows that in order to apply the electric field inside a crystal to measure the magnetic moment of baryons, in addition to the extremely strong electric field, the bending of the crystal along its planar direction is essential.

In sect. 2 we will briefly describe some characteristic aspects of crystals related with our subject, channeling phenomena, and calculate the electric field strengths for several crystal planes and axes. In sect. 3 we will calculate the magnitude of the precession angle of the polarization vector due to the electric field around the plane and axis of an unbent crystal. In sect. 4 we will discuss the bending effect of a crystal on the magnitude of the precession angle of the polarization vector.

2. Channeling and the crystal field

When a positively charged energetic particle approaches a crystal axis or plane at an angle smaller than a certain characteristic value, it experiences a successive series of correlated gentle Coulomb collisions with the atoms along the corresponding axis or plane and thus avoids the high-density region of the atoms while traveling through the crystal. This directional effect on the motion of the particle controlled by the crystal axes or planes is called particle channeling and has been a subject of extensive study in solid state physics with low-energy particle or ion beams [18, 19].

Since the mid-seventies, several channeling experiments with high-energy particle beams have been carried out, and succeeded in producing observable channeling effects of up to 250 GeV [20, 21]. It has been suggested by Tsyganov [22] and has been experimentally confirmed [23, 24] by using Si crystals that high-energy charged particles channeling between major crystal planes can be guided along bent crystal planes, thus making it possible to change the direction of the high-energy particles. The bending effect is simply due to very strong electric fields around the crystal planes or axes. Although the electric field strength depends on the kind of crystal and on the specific plane or axis concerned, the values are of the order of 10^{10} V/cm.

The characteristic angle which distinguishes the channeled and non-channeled particles is called the critical angle and is defined at high energy as

$$\psi_a = \sqrt{\frac{4Z_1Z_2e^2}{\epsilon d_a}}, \quad (1)$$

for the axes, and

$$\psi_p = \sqrt{\frac{4Z_1Z_2e^2Nd_pCa}{\epsilon}}, \quad (2)$$

for the planes, where ϵ is the relativistic energy of the particle, Z_1 the charge of the

TABLE 2
Characteristic constants of crystal

Crystal Constant	Si	Ge	W	Pt
charge	14	32	74	78
atomic weight	28.09	72.59	183.85	195.09
screening distance	0.1864	0.1407	0.1086	0.1068
atoms/ \AA^3	0.0499	0.0442	0.0631	0.0660
Debye temperature ($^{\circ}\text{K}$)	543	290	310	225
thermal amplitude (293 $^{\circ}\text{K}$)	0.075	0.085	0.050	0.066
thermal amplitude (150 $^{\circ}\text{K}$)		0.063	0.0373	0.0486
plane width (\AA)	1.920	2.000	2.238	2.2649
	(110)	(110)	(110)	(111)
atomic spacing (\AA)	3.840	4.000	2.741	2.774
	$\langle 110 \rangle$	$\langle 110 \rangle$	$\langle 111 \rangle$	$\langle 110 \rangle$

incident particle with Z_2 the proton number of the atoms in the crystal, d_a the atomic spacing along the corresponding axis, d_p the separation between adjacent planes, N the volume density of atoms, a the screening distance and C is a constant related to the screening which normally has a value $C = \sqrt{3}$. Some of the important characteristic constants of Si, Ge, W and Pt crystals are listed in table 2 and critical angles in table 3.

It has been demonstrated by Lindhard [18] that channeling phenomena can be satisfactorily explained by the classical continuum model, where the potentials due to individual atoms are averaged along the axis or plane. The accuracy of the model increases as the energy of the particle increases [25]. One of the most important assumptions of the continuum model is the approximate conservation of the transverse energy of channeled particles. If we neglect multiple scattering by the electrons and atoms displaced from the lattice site due to the vibrations, which tends to increase the transverse energy of the channeled particles, conservation of transverse energy of the channeled particles is accurate for particles with incident angle ψ_{in} less than the critical angle. However the effects of multiple scattering by both

TABLE 3
Critical angles of crystals (unit in μrad)

Crystal GeV	Si		Ge		W	Pt		
	$\langle 110 \rangle$	(110)	$\langle 110 \rangle$	(110)	$\langle 111 \rangle$	(110)	$\langle 110 \rangle$	(111)
100	45.8	15.8	67.9	19.9	124.7	33.6	127.3	35.2
200	32.4	11.2	48.0	14.1	88.2	23.7	90.0	24.9
300	26.5	9.12	39.2	11.5	72.0	19.4	73.5	20.3
400	22.9	7.90	33.9	10.0	62.3	16.8	63.6	17.6
500	20.5	7.10	30.4	8.90	55.8	15.0	56.9	15.8

electrons and displaced atoms on the trajectories of channeled particles have been detected experimentally [20, 21] and are also predicted by theory. A typical theoretical treatment of these effects is based on the diffusion theory of particles [26–28].

When the transverse energy of a channeled particle is increased beyond a critical energy, the particle penetrates into the region where the density of the lattice atoms is high and thus may have close collisions with one or several atoms, which causes the particle to change its trajectory violently, thus leading to non-conservation of transverse energy in the sense of the continuum potential model and eventually leads to the dechanneling of the particle.

As will be explained later we are primarily interested in planar channeling, and the continuum potential which describes planar channeling can often be rather well approximated by a simple harmonic potential. The simple harmonic potential is defined as

$$U(x) = V_0 x^2, \tag{3}$$

where $x = 0$ is the midpoint between the atomic planes. The discussion of more realistic potentials can be found in several references [19, 29, 30]. The coefficients V_0 of several different crystals are listed in table 4, along with the electric fields calculated at $\frac{1}{2}d_p$. Because of thermal vibrations, eq. (3) is not strictly valid up to $\frac{1}{2}d_p$ as shown in fig. 1. Therefore, the values of $E(x)$ at $\frac{1}{2}d_p$ given in table 4 should be considered as maximum values for each corresponding plane.

For region II in fig. 1, which is taken from ref. [31], $E(\frac{1}{2}d_p)$ is approximately calculated for the Si crystal and given by

$$E(\frac{1}{2}d_p) \sim 2.5 \times 10^9 \text{ V/cm}. \tag{4}$$

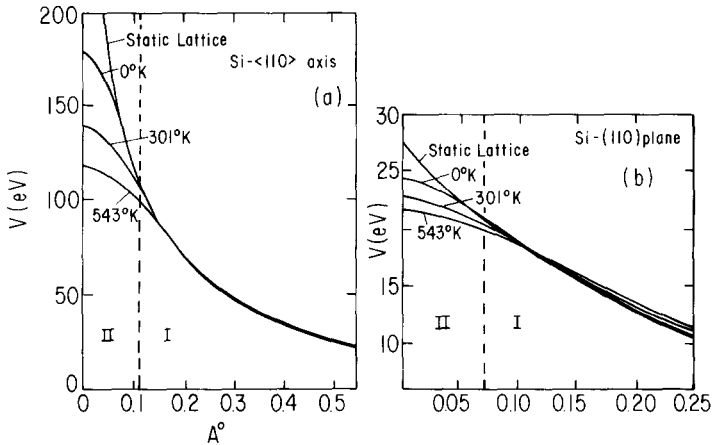


Fig. 1. Continuum potentials of Si crystal based on the Molière potential model, ref. [31]: (a) is for the $\langle 110 \rangle$ axis and (b) is for the (110) planes.

TABLE 4
 V_0 and $E(\frac{1}{2}d_p)$ for crystal planes

Crystal plane	V (V/Å ²)	$E(\frac{1}{2}d_p)$ (V/Å)
Si (110)	29.33	56.3
Ge (110)	45.30	99.5
W (110)	126.1	282.2
Pt (111)	126.2	307.8

Evidence from realistic models, like the Molière potential, as well as experimental evidence suggest that in the region close to the plane but still inside region I in fig. 1, the electric field seems to be stronger than that suggested by the simple harmonic potential model. However, as mentioned before, we will continue to use a harmonic potential for the crystal planar potential throughout the rest of this paper. This will tend to underestimate the precession of the polarization.

3. Precession of the polarization vector

If the expectation value of the spin component of a particle has a non-zero maximum value S in a certain direction e_0 , the particle is polarized and the polarization vector of the particle is defined as

$$\mathbf{S} = e_0 S = e_0 \langle \boldsymbol{\sigma} \cdot \mathbf{e} \rangle, \quad (5)$$

where $\boldsymbol{\sigma}$ is the intrinsic spin of the particle. The magnitude of the polarization S is known to be a constant of the motion but its direction changes in an electromagnetic field.

If a baryon C is produced in a parity-conserving interaction by unpolarized beam particles, the polarization vector \mathbf{S}_C of particle C is normal to the interaction plane formed by the incident particle momentum \mathbf{k}_{in} and the outgoing particle C momentum \mathbf{k}_{out} , i.e.

$$\mathbf{S}_C // \mathbf{k}_{in} \times \mathbf{k}_{out}. \quad (6)$$

For the remainder of the discussion, we assume that the particles we are interested in are produced with polarization. If the baryon C goes through a magnetic field perpendicular to the polarization \mathbf{S}_C before it decays, then the precession angle ϕ of the polarization vector \mathbf{S}_C is expressed as

$$\phi = \mu_C \frac{e}{M_p \beta_C} f(\mathbf{H}), \quad (7)$$

where $f(\mathbf{H})$ is a function of the magnetic field \mathbf{H} . ϕ can be determined by measuring the components of \mathbf{S}_C , which can be deduced from the emission angular distribution of the final protons [32]. The magnetic moment μ_C is then given as the gradient of the function in eq. (7), if we know the function $f(\mathbf{H})$. In the following discussion, we will study the function $f(\mathbf{H})$ due to the crystal field.

3.1. PRECESSION ANGLE OF THE POLARIZATION VECTOR

The polarization vector \mathbf{S} , like the other expectation values of quantum observables, will follow classical equations of motion. Classical relativistic equations of motion of spinor particles have been studied by several authors, typically by Bargmann et al. [33] for a homogeneous external electromagnetic field and by Good [34] for an inhomogeneous external field including up to first-order field-gradient effects by using a four-vector description of the polarization.

As has been discussed before, the electromagnetic field inside the crystal is very inhomogeneous. Along a crystal axis, the electric field is not only inhomogeneous, but also the direction is radially outward from each string. Therefore, the influence on the polarization vector will be different from particle to particle because of different azimuthal impact positions relative to the axis and this makes it impossible to apply the axial field to measure the polarization of the beam. For atomic planes, the electric field is also inhomogeneous, but its direction is parallel all over the crystal and is well approximated by a simple harmonic potential. Moreover, its effect on the direction of change of the polarization vector will not change from particle to particle as will be shown in sect. 4. We will therefore concentrate only on the planar field.

In order to study the polarization of a particle, it is convenient to have covariant expressions for the equations of motion. In general, the equation of motion of the polarization vector \mathbf{S} in the rest frame is

$$\frac{d\mathbf{S}}{dt} = g\mu\mathbf{S} \times \mathbf{H}^*, \quad (8)$$

where \mathbf{H}^* is the magnetic field in the rest frame of the particle. Its covariant form, given in ref. [35], is

$$\dot{S} = g\mu [SF - V(SFV)] - V(S\dot{V}), \quad (9)$$

where $S = (s_0, \mathbf{s})$, $S = (0, \mathbf{s}_R)$ in the rest frame, $V = \gamma(1, \boldsymbol{\beta})$, F is the anti-symmetric electromagnetic field tensor, $\boldsymbol{\beta} = \mathbf{v}/c$ and its derivative is taken over proper time. If two unit vectors \mathbf{n} and $\mathbf{l} = \boldsymbol{\beta}/\beta$ perpendicular to each other are defined such that the polarization vector in the rest frame \mathbf{S}_R lies in the plane spanned by \mathbf{n} and \mathbf{l} , the covariant expression for the precession rate of the polarization vector can be written

as [35]

$$\dot{\theta}_R = \dot{L}N - g\mu LFN \tag{10}$$

$$= \frac{1}{\beta} N\dot{V} - g\mu LFN. \tag{11}$$

where $\theta_R = \angle(s_R, \beta)$, $L = \gamma(\beta, l)$ and $N = (0, \mathbf{n})$. Since the first term is due to the angular change of the vector l , these equations express the precession rate of the polarization vector relative to the particle momentum vector in the rest system of the particle in covariant form.

3.2. PERIODIC CANCELLATION OF $\Delta\theta_R$ IN AN UNBENT CRYSTAL

Fig. 2a shows the trajectory of a positively charged particle channeling through a planar channel of an unbent crystal. Since the electric field is symmetric about the

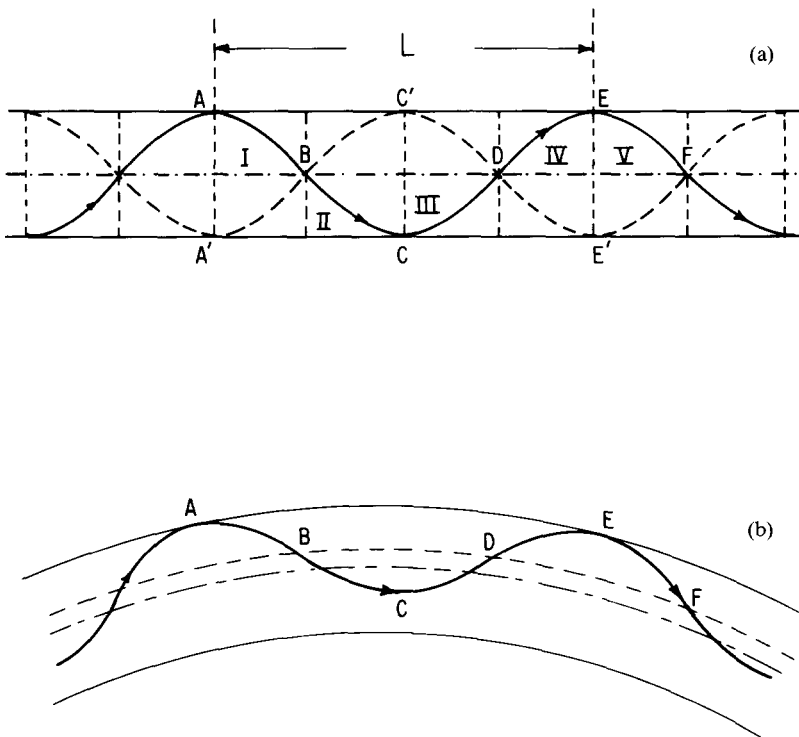


Fig. 2. Channeling particle's trajectory through crystal planes: (a) is for unbent crystal and (b) is for bent crystal planes.

central line of the planar channel, the trajectory itself is also symmetric. The precession angle of the polarization vector $\Delta\theta_R$ can be obtained by solving eq. (11) when a proper equation for \dot{V} is given.

When the electric field is inhomogeneous and $H = 0$, Good [34] derived the equation of motion of the particle as

$$\frac{d\mathbf{P}}{dt} = e\mathbf{E} + \mu\gamma^2[\nabla + \boldsymbol{\beta} \times (\boldsymbol{\beta} \times \nabla)]\mathbf{S} \cdot (\mathbf{E} \times \boldsymbol{\beta}), \quad (12)$$

which includes corrections up to first order of the gradient of \mathbf{E} . For the simple harmonic potential,

$$\nabla\mathbf{S} \cdot (\mathbf{E} \times \boldsymbol{\beta}) = 2V_0S_y\mathbf{i}, \quad (13)$$

where $\mathbf{i} = \mathbf{l} \times \mathbf{n}$. By substituting this result into eq. (11), one can easily solve it for $\Delta\theta_R$. This solution shows that there are additional non-zero contributions to $\Delta\theta_R$ from the inhomogeneous field.

However, since we are interested in very high energy particles which are channeling through a crystal planar channel and the planar critical angle is very small as indicated in table 3, $\boldsymbol{\beta}$ should be almost parallel to the crystal planar direction in order for the particle to channel. Moreover, in order to produce very high energy secondary particles, the momentum of the incident beam particle should be very large and almost parallel to the crystal planar direction, since the production cone would be very narrow. Therefore, the interaction plane will be almost parallel to the crystal plane and the polarization vector \mathbf{S} will be nearly perpendicular to the crystal plane and will satisfy the condition

$$\nabla\mathbf{S} \cdot (\mathbf{E} \times \boldsymbol{\beta}) \approx 0. \quad (14)$$

We can therefore neglect the interaction term of \mathbf{S} with \mathbf{E} in eq. (12) which then turns out to be the same equation of motion as that of a polarized particle subjected to a homogeneous electromagnetic field. Under this condition, eq. (11) becomes

$$\frac{d\theta_R}{dt} = \frac{e}{2mc} \left[(g-2) - \frac{g}{\gamma^2} \right] (\mathbf{E} \cdot \mathbf{n}), \quad (15)$$

which is a well-known equation for the case of a homogeneous field.

The total precession angle of \mathbf{S} over the trajectory can be obtained by integrating eq. (15) over time. However, since \mathbf{E} is symmetric about the central line in fig. 2a, most of the contributions to $\Delta\theta_R$ in successive half-cycles cancel. The maximum $\Delta\theta_R$ will therefore be produced over a single half-cycle of the motion. $\Delta\theta_R$ in eq. (15) can

be expressed in terms of the transverse momentum transfer of the particle as

$$\Delta\theta_R = \frac{1}{2m\beta c} \left[(g-2) - \frac{g}{\gamma^2} \right] \Delta p_{\perp}. \quad (16)$$

When eq. (14) is satisfied, the interaction term of \mathbf{S} with \mathbf{E} is negligible and the conservation of transverse energy in the channeling is given by

$$\varepsilon_{\perp} = \frac{1}{2}pv\psi^2 + eU(x), \quad (17)$$

where ψ is the angle of β relative to the planar direction. The maximum Δp_{\perp} in eq. (16) can then be expressed in terms of the critical angle, which results in

$$\Delta\theta_R = -\frac{1}{2} \frac{\gamma}{\beta} \left[(g-2) - \frac{g}{\gamma^2} \right] \psi_p. \quad (18)$$

This gives $\Delta\theta_R$ over a quarter period of the motion and although its value depends on many factors, its maximum is only of the order of mrad, which is not large enough to allow a reliable measurement of the magnetic moment. If we substitute eq. (2) for ψ_p , we find the dependence of $\Delta\theta_R$ on γ , Z_2 as

$$\Delta\theta_R \sim \sqrt{\gamma Z_2}. \quad (19)$$

From eq. (19) we can conclude that the larger the Z_2 of the crystal and the higher the energy of the incident particle, the larger the precession angle $\Delta\theta_R$ will be. This is easy to understand because high Z_2 means a stronger electromagnetic field and higher energy means a larger time dilatation factor in the Lorentz transformation.

4. Bending effect on the polarization vector

The discussion of sect. 3 reveals that the periodic cancellation of the contribution to $\Delta\theta_R$ due to the electric field of the opposite plane severely limits the magnitude of $\Delta\theta_R$. This limitation can be overcome by using a bent crystal. The major change introduced by bending the crystal is that a centrifugal term is introduced into the effective potential and this shifts the equilibrium position of the trajectory away from the symmetry point of the potential as shown in fig. 2b. The shift of the trajectory not only reduces the periodic cancellation of $\Delta\theta_R$, but also allow $\Delta\theta_R$ to accumulate through many cycles while the particles are channeling along the bent track (fig. 2b). The magnitude of the accumulation will increase as bending curvature increases and as the length of the channeling trajectory through the bent crystal increases. However, as will be discussed later, increasing the bending curvature effectively lowers the height of the effective potential-well and results in a reduction

of the number of particles channeling through the bent crystal. Increasing the length of the bent crystal is also limited by the lifetime of the short-lived particle and by the dechanneling phenomena. These conflicting effects force a compromise in the crystal bending curvature and length. Since the effect of bending on the track of the positive particles and negative particles differs significantly and the simple harmonic potential model is not a good approximation for negative particles, in this report we will confine ourselves to positive particles only.

4.1. BENDING EFFECT ON THE TRAJECTORY OF A POSITIVE PARTICLE

If a crystal is bent along one of the major directions with bending radius R and if the planar direction is properly aligned relative to the polarization direction so that eq. (14) is satisfied for the channeled particles, then we can neglect the interaction term of \mathbf{S} with \mathbf{E} and the equation of motion becomes

$$\frac{d^2x}{dz^2} + \frac{e}{pv} U'(x) + \frac{1}{R} = 0, \quad (20)$$

where the last term is the centrifugal term. This equation can be integrated to give

$$\varepsilon_{\perp} = \frac{1}{2}pv\psi^2 + eU(x) + \frac{pv}{R}x, \quad (21)$$

This is the modified equation of the transverse energy conservation for a particle channeling through bent planes. This equation suggests the modification of the effective potential as [36,37]

$$U^B(x) = eU(x) + \frac{pv}{R}x. \quad (22)$$

The centrifugal term introduces asymmetry in the effective potential such that it lowers the height of the outer potential wall while it increases the height of the inner wall when compared with the potential of the unbent crystal (fig. 3). This makes many particles, which would channel through if the crystal was not bent, dechannel when they enter into the bent crystal. In other words, any particle whose transverse energy ε_{\perp} satisfies

$$\varepsilon_{\perp}^{\text{BC}} < \varepsilon_{\perp} < \varepsilon_{\perp}^{\text{C}}, \quad (23)$$

will channel through the unbent crystal; but when it is incident on the bent crystal it will dechannel. $\varepsilon_{\perp}^{\text{C}}$ is the critical transverse energy when the crystal is not bent and $\varepsilon_{\perp}^{\text{BC}}$ is the critical transverse energy when it is bent. Those dechanneled particles will cross over the outer plane and will not follow the bent trajectory. Some model calculations have been carried out to estimate the dechanneling fraction due to

crystal bending [36, 37]. If we use the simple harmonic potential for $U(x)$, then the effective potential will be

$$U^B(x) = V_0(x^2 + ux), \tag{24}$$

where the new variable u is defined as

$$u = \frac{1}{eV_0} \frac{pv}{R}. \tag{25}$$

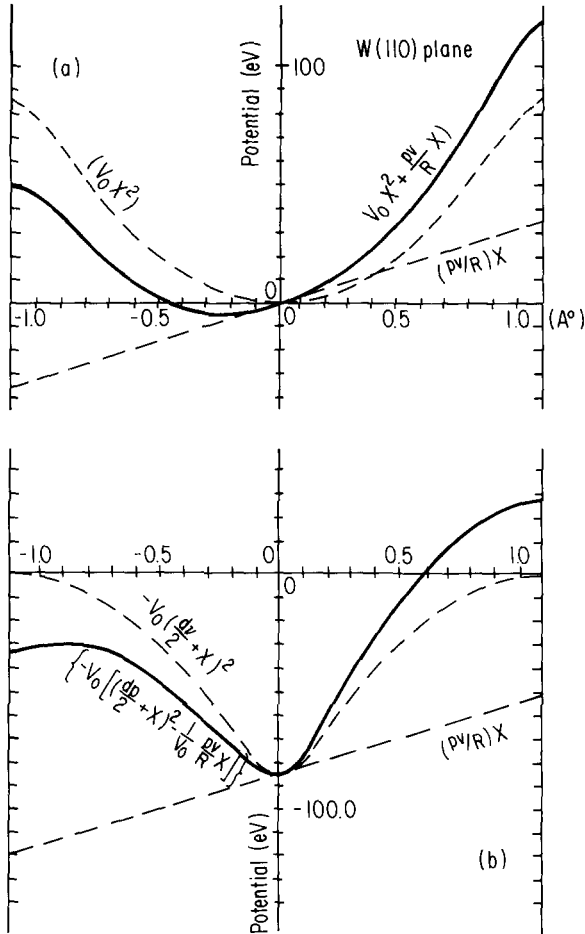


Fig. 3. Modified continuum (110) planar potential of bent tungsten: (a) is for the positive particle where $x = 0$ is in the central position between two adjacent planes and (b) is for the negative particle where $x = 0$ is a planar position.

By using the variable u , many equations in the following discussion can manifestly show their universal character in the sense that it can be easily applied to different crystals. Eq. (24) indicates that the period of the motion is not affected by the bending of the crystal, but the equilibrium position of the trajectory is shifted from $x = 0$ to $x = -\frac{1}{2}u$ for the simple harmonic model.

If the total transverse energy ϵ_{\perp} is smaller than the energy corresponding to the maximum height of the bent crystal potential, the particle will remain channeled and the particle trajectory will be confined between $x_L < x < x_H$ in the channel as shown in fig. 2b. The minimum and maximum transversal position in the channel can be obtained from eq. (21) and given as

$$x_L = \frac{1}{2}(-u - \sqrt{u^2 + 4w}), \tag{26}$$

$$x_H = \frac{1}{2}(-u + \sqrt{u^2 + 4w}), \tag{27}$$

where $w = \epsilon_{\perp}/V_0$. Thus the particle oscillates with amplitude $a = \frac{1}{2}\sqrt{u^2 + 4w}$, around the equilibrium position $x = -\frac{1}{2}u$ in a transverse motion confined to $x_L < x < x_H$.

4.2. BENDING EFFECT ON THE PRECESSION ANGLE $\Delta\theta_R$

The precession of the polarization vector \mathbf{S} is determined by the electric field, and not by the centrifugal field. The electric field around the bent plane is still symmetric around $x = 0$, and only part of the contribution to $\Delta\theta_R$ from $x_L < x < 0$ is cancelled by the contribution from $0 < x < x_H$. The remaining contribution to $\Delta\theta_R$ will accumulate while the particle channels through the bent crystal following the track shifted towards the outer plane.

To find the $\Delta\theta_R$ of the particle channeling through the bent crystal plane, we can neglect the interaction between \mathbf{S} and \mathbf{E} for the channeling particle and \dot{V} in eq. (11) can be substituted by

$$\dot{V} = -\frac{e}{mc}F'V, \tag{28}$$

where $F'(x)$ is the modified field derived from eq. (24), which differs from $F(x)$ derived from eq. (3). Then eq. (11) becomes

$$\dot{\theta}_R = -\frac{e}{m\beta c}NF'V - guLFN. \tag{29}$$

Simple integration shows that the contribution from the first term in eq. (29) comes from crystal bending. As explicitly expressed in eq. (10), the first term is due to the change in direction of $\mathbf{l} = \boldsymbol{\beta}/\beta$ and can be obtained by measuring the bending angle of the crystal over the trajectory.

If we use the following relation

$$\dot{N} = -\gamma \mathbf{n} \cdot \mathbf{l}, \quad (30)$$

and F is expressed in terms of E , we obtain

$$\Delta\theta_R = g\mu\beta \int \mathbf{E} \cdot \mathbf{n} dt + \gamma \frac{v}{R} \Delta t, \quad (31)$$

where the second term gives the bending angle of the crystal over the crystal length $v \cdot \Delta t$. The time interval dt can be expressed as

$$dt = \frac{dp_{\perp}}{F'(x)}, \quad (32)$$

where $F'(x)$ is obtained from eq. (24) and dp_{\perp} from eq. (21). Then a simple calculation gives us the expression for $\Delta\theta_R$ as

$$\Delta\theta_R = -g\mu\beta \sqrt{\frac{2m\gamma v_0}{e}} \frac{\pi}{2} u + \frac{\gamma v \Delta t}{R}. \quad (33)$$

$\Delta\theta_R$ is the change in the angle between the polarization vector and the velocity of the particle measured in the rest frame during one half period of the motion of the particle along the plane. Then $\Delta\theta_R^{\tau}$ over the particle lifetime τ is given by

$$\Delta\theta_R^{\tau} = \frac{1}{2}\gamma \left[(2-g) - \frac{g}{\gamma^2} \right] \frac{\gamma v \tau}{R}, \quad (34)$$

where use has been made of the relation for the period given by

$$T = 2\pi \sqrt{\frac{m\gamma}{2eV_0}}. \quad (35)$$

This equation is exactly the same as in the case when the electromagnetic field is homogeneous. However, this derivation is based on the assumption that for the particles channeling through a bent crystal, the potential is well approximated by a simple harmonic potential and the contribution to the particle motion from the interaction of S with E is negligible for channeling particles. From eq. (34), we can deduce the relation

$$\Delta\theta_R^{\tau} \sim \frac{1}{\sqrt{V_0}} \frac{\gamma^{3/2}}{R}. \quad (36)$$

Eq. (36) is equivalent to eq. (19) since $V_0 \sim Z_2$ and also indicates that as the particle energy is higher and the crystal is heavier, the precession angle $\Delta\theta_R^{\tau}$ becomes larger.

In order to calculate the expected order of $\Delta\theta_R^\tau$, we will use the definition of the magnetic moment

$$\mu = \frac{1}{2}g \frac{q\hbar}{2mc} . \tag{37}$$

Then eq. (34) becomes

$$\Delta\theta_R^\tau = \left[1 - \mu \frac{m}{m_p} \beta^2 \right] \frac{\gamma^2 v}{R} \tau , \tag{38}$$

where μ is given in units of nuclear magnetons ($\mu_N = e\hbar/2m_p c$). While the factor $A = 1 - \mu m/m_p \beta^2$ in eq. (38) is very sensitive to the value of the magnetic moment μ , the factor $B = \gamma^2 v \tau/R$ depends on the particle energy, its lifetime and the bending radius of the crystal. For the standard static quark model for spin- $\frac{1}{2}$ baryons the magnetic moment is given by [39]

$$\mu = \frac{1}{3}(2\mu_1 + 2\mu_2 - \mu_3) , \tag{39}$$

where μ_i is the constituent quark magnetic moment. If the baryons are flavor degenerate, then the second one is given by

$$\mu' = \mu_3 . \tag{40}$$

We will assume the following values for the quark magnetic moment [39]

$$\begin{aligned} \mu_u &= -2\mu_d = 1.86 , \\ \mu_s &= -0.61 , \quad \mu_c = 0.39 . \end{aligned} \tag{41}$$

These can be obtained from eq. (37) by assuming they are point-like and assigning them a proper mass. We can then calculate the magnetic moment of $\Lambda_c^+(udc)$ by replacing μ_1, μ_2 with μ_u, μ_d and μ_3 by μ_c in eq. (39). However, since Λ_c^+ forms a flavor degenerate pair with Σ_c^+ in the baryon octet weight diagram, we use eq. (39) for $\mu_{\Sigma_c^+}$ and eq. (40) for $\mu_{\Lambda_c^+}$. Then we obtain

$$\mu_{\Sigma_c^+} = 0.49 , \tag{42}$$

$$\mu_{\Lambda_c^+} = 0.39 . \tag{43}$$

A model calculation [37] shows that for particles with momentum 300 GeV/c, the dechanneling fraction due to the bending of the (110) plane of tungsten with $R = 30$ cm is only about 30%. Therefore, in a practical sense, the limit on the bending radius of the crystal will be decided by the mechanical properties of the crystal.

We will calculate $\Delta\theta_R^\tau$ for several particles to show the magnitude of the expected precession angle of the polarization vector. Assuming that $\mu_{\Lambda_c^+} = 0.39$, $mc^2 = 2.273$ GeV and $\tau_{\Lambda_c^+} = 2.0 \times 10^{-13}$ sec, we will get $\Delta\theta_R^\tau$ for Λ_c^+ when $R = 30$ cm and $\gamma = 200$

$$\Delta\theta_R^\tau = 0.44 \text{ rad.} \quad (44)$$

For Σ_c^+ , if we assume that $\mu_{\Sigma_c^+} = 0.49$ and $mc^2 = 2.44$ GeV [40], under the same conditions as above, we will get

$$\Delta\theta_R^\tau = -1.1 \times 10^{13} \tau. \quad (45)$$

Therefore, $\tau = 10^{-13}$ sec will give us about $\Delta\theta_R^\tau = 1$ rad. For Ξ_c^+ (usc), if we use $\mu_{\Xi_c^+} = 0.7$ [39] and $mc = 2.5$ GeV, under the same conditions as above, we will get

$$\Delta\theta_R^\tau = -3.6 \times 10^{13} \tau. \quad (46)$$

However, there are ambiguities in obtaining $\mu_{\Xi_c^+}$, since there is no guiding principle such as isospin symmetry to decide the quark ordering for Ξ_c^+ . If one uses a charmed quark as the third quark in eq. (39), then $\mu_{\Xi_c^+} = 0.7$. However, if one uses a u-quark as the third quark, then $\mu_{\Xi_c^+} = -0.77$ [39]. These are about the same magnitude but have opposite sign. Therefore, the accurate measurement of $\mu_{\Xi_c^+}$ could supply us very important information on quark ordering in eq. (39), if the equation is still valid. For a particle including a bottom flavored quark, Ξ_{cb}^+ (ucb), if we use $\mu_{\Xi_{cb}^+} = 1.5$ [39], $mc^2 = 7$ GeV and $R = 30$ cm, we could achieve

$$\Delta\theta_R^\tau = -38 \times 10^{13} \tau. \quad (47)$$

Therefore, for Ξ_c^+ and Ξ_{cb}^+ , even if the lifetime is much shorter than Λ_c^+ , we can achieve a very large precession angle $\Delta\theta_R^\tau$ over its lifetime even at much lower γ .

Finally, if we assume that a τ^+ lepton is produced in hadron-hadron scattering as a decay product of the F or B meson and also assume that it is polarized longitudinally, then eq. (34) can be applied without modification to calculate the precession angle of the τ^+ lepton polarization vector. However, if the τ^+ lepton behaves like a point particle and its anomalous magnetic moment does not deviate from that of the muon or electron, then eq. (34) suggests that γ of the τ^+ lepton should be larger than 1000 in order to show any appreciable effect on the final lepton asymmetry distribution.

5. Conclusion

We have shown that it should be possible to apply planar channeling phenomena to measure the magnetic moment of short-lived baryons with heavy flavored quarks. For such particles the magnitude of the precession angle $\Delta\theta_R^\tau$ of the polarization

vector of the particle, over its lifetime in the rest frame, is estimated to be of the order of radians. This assumes that the particles are produced with polarization and high γ . For the τ^+ lepton, unless its anomalous magnetic moment deviates from the value of μ or e , we would need a beam energy of the order of 10 TeV.

In order to reach this result, we have assumed that the inhomogeneous potential of the crystal plane can be approximated by a simple harmonic potential and that the crystal is aligned so that $\nabla\mathbf{S} \cdot (\mathbf{v} \times \mathbf{E}) = 0$. Even if the latter condition is not satisfied, for the simple harmonic potential approximation, the contribution due to non-zero value of $\nabla\mathbf{S} \cdot (\mathbf{v} \times \mathbf{E})$ is not significant mainly due to the short lifetime, the heavy mass of the baryons and the smallness of A in our case.

Although the exact magnitude of $\Delta\theta_R^\tau$ depends on many factors, by choosing an appropriate crystal and bending radius, we can measure the magnetic moment of short-lived particles with lifetimes of the order of 10^{-13} s. Moreover, by applying planar channeling through a bent crystal, we should be able to separate spatially most of the background particles produced at the same time [38].

Since we are approaching the tevatron age of the accelerator, the measurement of the magnetic moments of short-lived particles by planar channeling through a bent crystal might be feasible in the near future.

I would like to thank Prof. Lee Pondrom, who first pointed out the possibility of applying channeling phenomena in measuring magnetic moments, for very helpful conversations and critical suggestions. I express deep gratitude to my colleagues for many discussions, including Prof. C.R. Sun, Dr. R.A. Carrigan, Jr. and especially Prof. W.M. Gibson for his critical reading of the manuscript and advice. This work has been supported in part by the Department of Energy.

References

- [1] M. Goldhaber, Phys. Rev. 101 (1956) 1828
- [2] T.D. Lee and C.N. Yang, Phys. Rev. 108 (1957) 1645
- [3] G. Morpugo, Ann. of Phys. 2 (1965) 95
- [4] M.A. Beg and A. Pais, Phys. Rev. 137B (1965) 1514
- [5] H.R. Rubinstein, F. Scheck and R.H. Socolow, Phys. Rev. 154 (1967) 1608
- [6] J. Franklin, Phys. Rev. 182 (1969) 1607
- [7] A. De Rújula, H. Georgi and S.L. Glashow, Phys. Rev. D12 (1975) 147
- [8] O. Overseth, Proc. 4th Int. Conf. on Baryon resonances, Toronto, ed. N. Isgur (University of Toronto, 1981) p. 259
- [9] P. T. Cox, J. Dworkin, O.E. Overseth, R. Handler, R. Grobel, L. Pondrom, M. Sheaff, C. Wilkinson, L. Deck, L. Devlin, K.B. Luk, R. Rameika, P. Skubic, K. Heller and G. Bunce, Phys. Rev. Lett. 46 (1981) 877
- [10] L.L. Deck, Ph.D. thesis, Rutgers University (1981), unpublished
- [11] R. Rameika, Ph.D. thesis, Rutgers University (1981), unpublished
- [12] D.B. Lichtenberg, E. Predazzi and J.G. Wills, Indiana University report IUHET-75 (1982)
- [13] H.J. Lipkin, Phys. Rev. D24 (1981) 1437
- [14] S. Theberge and A.W. Thomas, Phys. Rev. D25 (1982) 284
- [15] T. Thomozawa, Phys. Rev. D25 (1982) 795

- [16] H. Harari, *Phys. Lett.* 86B (1979) 83
- [17] H.J. Lipkin, *Fermi-Pub-81/36-Thy*
- [18] J. Lindhard, *Mat. Fys. Medd. Dan. Vid. Selsk.* 34 (1965) 14
- [19] Donald S. Gemmel, *Rev. Mod. Phys.* 46 (1974) 129
- [20] R.A. Carrigan, Jr., B.L. Chrisman, T.E. Toohig, W.M. Gibson, Ick-Joh Kim, C.R. Sun, Z. Guzik, T.S. Nigmanov, E.N. Tsyganov, A.S. Vodopianov, M.A. Hasan, A.S. Kanofsky, R. Allen, J. Kubie, D.H. Stork and A.B. Watson, *Nucl. Phys.* B163 (1980) 1
- [21] S.K. Andersen, O. Fich, H. Nielsen, H.E. Schiøtt, E. Uggerhøj, C.V. Thomsen, G. Charpak, G. Petersen, F. Sauli, J.P. Ponpon, and P. Siffert, *Nucl. Phys.* B167 (1980) 1
- [22] E.N. Tsyganov, *Fermilab TM-682, TM-684, Batavia, 1976*
- [23] A.F. Elishev, N.A. Filatova, V.M. Golovatyuk, I.M. Ivanchenko, R.B. Kadyrov, N.N. Karpenko, V.V. Korenko, T.S. Nigmanov, V.D. Riabtsov, M.D. Shafranov, B. Sitar, A.E. Senner, B.M. Starchemko, V.A. Sutulin, I.A. Tyapkin, E.N. Tsyganov, D.V. Uralsky, A.S. Vodopianov, Z. Guzik, A. Forycki, J. Wojtkowska, R. Zelazny, I. Agrishaev, G.D. Kovalenko, B.I. Shramenko, M.D. Bavizhev, N.K. Bulgakov, V.V. Avdeichikov, R.A. Carrigan, Jr., T.E. Toohig, W.M. Gibson, Ick-Joh Kim, J. Phelps and C.R. Sun, *Phys. Lett.* 88B (1979) 387
- [24] J. Bak, G. Melchart, E. Uggerhøj, J. Forster, P.R. Jensen, H. Madsboll, S.P. Møller, H. Nielsen, G. Petersen, H. Schiøtt, J.J. Grab and P. Siffert, *Phys. Lett.* 93b (1980) 505
- [25] P. Lervig, J. Lindhard and V. Nielsen, *Nucl. Phys.* A96 (1967) 481
- [26] E. Bonderup, H. Esbensen, J.U. Andersen and H.E. Schiøtt, *Rad. Eff.* 12 (1972) 261
- [27] L.C. Feldman, B.R. Appleton and W.L. Brown, *Solid state phys. research with accelerator BNL-50083* (1968)
- [28] K. Morita, *Rad. Eff.* 14 (1972) 195
- [29] J.A. Ellison, E. Uggerhøj, J. Bak and S.P. Møller, *Phys. Lett.* 112B (1982) 83
- [30] G. Molière, *Z. Naturforsch.* A2 (1947) 133
- [31] B.R. Appleton, C. Erginsoy and W.M. Gibson, *Phys. Rev.* 161 (1967) 330
- [32] G. Bunce, O.E. Overseth, P.T. Cox, J. Dworkin, K. Heller, T. Devlin, B. Edelman, R.T. Edwards, L. Schachinger, P. Skubic, R. Handler, R. March, P. Martin, L. Pondrom and M. Sheaff, *Phys. Lett.* 86B (1979) 386
- [33] V. Bargman, L. Michel and V.L. Telegdi, *Phys. Rev. Lett.* 2 (1959) 435
- [34] R.H. God, Jr., *Phys. Rev.* 125 (1962) 2112
- [35] R. Hagedorn, *Relativistic kinematics* (Benjamin)
- [36] Hiroshi Kudo, preprint University of Tsukuba (1981)
- [37] J.A. Ellison, *Nucl. Phys.* B206 (1982) 205
- [38] R.A. Carrigan, Jr., *Fermilab-Pub-80/45-Exp* 7850.507
- [39] J. Franklin, D.B. Lichtenberg, W. Namgung and D. Carydas, *Phys. Rev.* D24 (1981) 2910
- [40] L.A. Copley, N. Isgur and G. Karl, *Phys. Rev.* D20 (1979) 768
- [41] R.B. Teese and R. Settles, *Phys. Lett.* 87B (1979) 111
- [42] R. Settles, A. Manz, W. Matt, T. Hansl, I. Herynek, N. Dobbie, G. Wolf, S. Reucroft, J. Marraffino, J. Watters, M. Webster and C.E. Roos, *Phys. Rev.* D20 (1979) 2154
- [43] G. Dugan, Y. Asano, M.Y. Chen, S.C. Cheng, E. Hu, L. Lidofsky, W. Patton, C.S. Wu, V. Hughes and D. Lu, *Nucl. Phys.* A254 (1975) 396
- [44] T. Devlin, *Bull. Am. Phys. Soc.* 25 (1980) 572
- [45] F. Dydak, F.L. Navarrian, O.E. Overseth, P. Steffen, J. Steinberger, H. Wahl, E.G.H. Williams, F. Eisele, C. Geveniger, K. Kleinknecht, H. Taureg and G. Zech, *Nucl. Phys.* B118 (1977) 1